THE JOURNAL OF PHYSICAL CHEMISTRY C

Article

pubs.acs.org/JPCC

Solvent Induced Adhesion Interactions between Dichlorotriazine Films

Iraklii I. Ebralidze,[†] Mohammad Hanif,[†] Rubaiyat Arjumand,[†] Alyza A. Azmi,[†,‡] Daniel Dixon,[†] Natalie M. Cann,[†] Cathleen M. Crudden,[†] and J. Hugh Horton*[,†]

[†]Department of Chemistry, Queen's University, Kingston, Ontario K7L 3N6, Canada

[‡]Department of Chemistry, Malaysia University of Terengganu, Terengganu 23000, Malaysia

Supporting Information

ABSTRACT: This article reports adhesion interactions between silicon-supported dichlorotriazine films in various solvents. The formation, chemical composition, and thickness of the overlayer were analyzed by means of X-ray photoelectron spectroscopy (XPS). An atomic force microscopy (AFM) characterization was performed to evaluate the overlayer roughness. Adhesion interactions were measured using chemical force spectrometry (CFS). The purpose of the study is to understand the effect of solvents on the adhesion force between dichlorotriazine films. The tip−surface adhesion forces measured in octane and cyclooctane were found to be relatively weak. Use of solvents that may participate in $\pi-\pi$ interactions, such as toluene and trifluoromethyl benzene, as well as a potential monohalogen bond donor, such as CCl_4, did not lead to significant increase in the tip−surface forces. However, the adhesion forces increase considerably when measured in solvents that contain at least two ether groups, such as dioxane, diethylene glycol dimethyl ether, and triethylene glycol dimethyl ether. These most important interactions in ether-type solvents are due to bridging of the solvent between the two surfaces. Molecular dynamics simulations of the functionalized surfaces are consistent with enhanced solvent bridging interactions when the solvent contains ether functional groups.

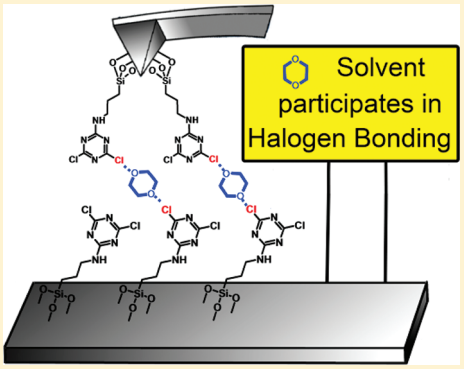

1. INTRODUCTION

The utilization of molecules that can form multiple interactions with their neighbors[1,2] by combination of their $\pi-\pi$ stacking abilities with other noncovalent interactions, such as hydrogen and halogen bonds is a productive strategy in crystal engineering.[3] These interactions are based on the transfer of charge density. Thus, hydrogen bonding can be viewed as a noncovalent force arising from the electrostatic interactions between an electronegative donor group that is covalently bound to a hydrogen atom and an electron acceptor.[4] A related, although less commonly observed noncovalent interaction is halogen bonding.[3] This type of bonding describes interactions between the electropositive portion of a halogen atom and the negative electron cloud of a heteroatom. The existence and magnitude of the positive region, known as the σ-hole, depends on the relative electron-attracting power of the halogen and the remainder of the molecule. Among other effects, the surface of the σ-hole increases when the carbon atom bound to the heavy halogen atom is also connected to other electronegative species.[5]

Recently, halogen bonding has been shown to be a useful tool in the development of nonlinear optical devices, polymer coatings, separation technologies, and the formation of supramolecular assemblies.[6] Much progress has been made in demonstrating the potential of halogen-bonding, as evidenced by the recent work of Resnati and Metrangolo,[2,3,7−9] van der Boom,[10−12] and others.[13−17] Nevertheless, the vast majority of halogen-bonded systems involve cocrystallization of separate donor- and acceptor-containing molecules. By contrast, examples of bifunctional compounds containing both halogen donor and acceptor parts are relatively rare.[6] Chloro-containing 1,3,5-triazines are simple and elegant examples of such bifunctional compounds. Derivatives of 1,3,5-triazine[18−20] as well as their metal complexes[21,22] have shown great potential in molecular recognition and in the formation of supramolecular architectures due to both their π-interaction abilities and for their propensity to be involved in intricate H-bond networks. Thus, chlorinated 1,3,5-triazine derivatives are intriguing because of their potential to form Cl···N halogen bonds.[23,24]

In this article, we report on the use of the chemical force spectrometric (CFS) method to study the adhesive interations between a 4,6-dichloro-1,3,5-triazine modified silicon wafer with a silicon cantilever tip that was also modified by a 4,6-dichloro-1,3,5-triazine film. Dichlorotriazines can potentially interact via halogen bonding and $\pi-\pi$ stacking. Interaction forces were measured in a variety of organic solvents containing halogen, aromatic, or ether groups. Molecular dynamics simulations of pairs of functionalized surfaces in the presence of solvent provide insight into the physical origin of the measured forces. To the best of our knowledge, there is only

Received: November 29, 2011
Revised: December 22, 2011
Published: January 18, 2012

   dx.doi.org/10.1021/jp211503x | J. Phys. Chem. C 2012, 116, 4217−4223

one report of a chemical force measurement for a halogen-bonded system.[25] Because of the relatively small size of the crystals used in those experiments and challenges arising from limited solubility, the adhesion forces were measured in air. In our work, we have chosen to explore the effect of solvent on the interactions between 4,6-dichloro-1,3,5-triazine overlayers. While solvent may significantly reduce the magnitude of the halogen bonding interaction,[26] CFS measurements carried out in solvents preclude any influence of capillary forces arising from water that might be adsorbed on the surface.[27]

2. EXPERIMENTAL SECTION

The synthesis of (3-(4,6-dichloro-1,3,5-triazin-2-yl)propyl)-siloxane was accomplished in two steps. In the first step, 3-aminopropyltriethoxysilane (**1**) was reacted with cyanuric chloride (**2**) (see Scheme 1). The resulting compound **3** was

Scheme 1. Synthesis and Deposition of 2,4-Dichloro-6-(3-(triethoxysilyl)propyl)-1,3,5-triazine on Si(111) Surface

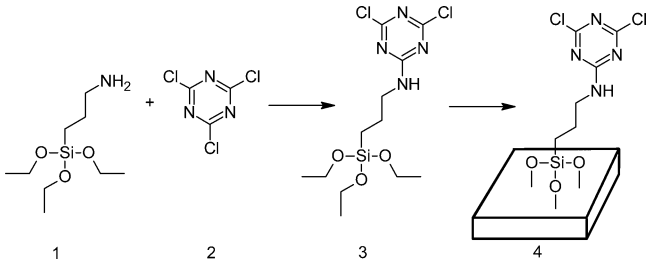

isolated and fully characterized. The second step involved deposition of **3** on an oxidized silicon surface (see the Supporting Information for details).

Single-crystal silicon [111] substrates, purchased from Wafernet (San Jose, CA), were precleaned by sonication in hexane followed by acetone and then ethanol and dried under an N_2 stream followed by immersing in a hot (70 °C) piranha solution (7:3 (v/v) H_2SO_4/30% H_2O_2) for 1 h. *Caution! Piranha solution is an extremely dangerous oxidizing agent and should be handled with care using appropriate personal protection.* The substrates were then rinsed with deionized water followed by the RCA cleaning protocol: 1:5:1 (v/v) $NH_3{\cdot}H_2O/H_2O/30\%$ H_2O_2 at room temperature for 45 min.[28] The substrates were subsequently washed with deionized water and dried under an N_2 stream and then in an oven for 2 h at 130 °C. Ultrasharp silicon cantilevers with a tip radius of ~10 nm purchased from MikroMasch, Estonia. Gold coated mica substrates were purchased from Georg Albert PVD, Germany. Cr–Au coated silicon tips CSC38/Cr–Au were purchased from MikroMasch, U.S.A. Gold-coated surfaces were cleaned by sonication in hexane followed by acetone and then ethanol and dried under an N_2 stream. Monolayer formation was carried out using dry solvents under an inert atmosphere using standard Schlenk/cannula techniques and/or an N_2-filled glovebox.

Freshly cleaned and dried oxidized silicon substrates (1 cm × 1 cm) or silicon tips were loaded with a freshly prepared 21 mM solution of 2,4-dichloro-6-(3-(triethoxysilyl)propyl)-1,3,5-triazine (3) in dry cold (0 °C) dichloromethane and held at 3 °C in a sealed nitrogen-filled vessel for 3 h. The functionalized substrates were then rinsed repeatedly with dry dichloromethane and sonicated in dry dichloromethane 2 times for 6 min each. The substrates were predried under a stream of N_2, left in high vacuum for 8 h, and held in anhydrous atmosphere.

To form SAMs of 12-morpholinododecane on gold, Au-coated mica substrates (1 cm × 1 cm) were annealed with methane flame followed by immersion in 1 mM methanol solution containing 12-morpholinododecane-1-thiol for 24 h at room temperature. The modified tips and substrates were rinsed repeatedly with absolute methanol and deionized water. The substrates were predried under a stream of N_2, left in high vacuum for 8 h, and held in anhydrous atmosphere.

Force–distance curves were acquired using a PicoSPM (Molecular Imaging, Tempe, AZ) and a Nanoscope IIE controller (Digital Instruments, Santa Barbara, CA). All experiments were carried out at 20 °C. The adhesive force between the tip and sample was measured from the average of the adhesive well depth of 200–300 force–distance curves in each solvent. The reported values of the adhesive interaction are an average of all of the adhesive forces, and the reported errors reflect the standard deviation of the data. The adhesive force between the tip and substrate was remeasured several times between the same tip and different surface sites.

Molecular dynamics (MD) simulations were performed for (3-(4,6-dichloro-1,3,5-triazine)propyl) siloxane (DCTPS) interfaces. Within the simulation cell, each surface has a 37.44 Å × 37.44 Å surface area and consists of an immoveable layer of Si with silanol groups, at a coverage of 8.2 μmol/m^2, and DCTPS with a coverage of 1.1 μmol/m^2. Simulations are conducted for surfaces separated by 56, 42, 35, 28, and 24 Å. In order to employ 3D periodic boundary conditions and yet examine fluid confined between two surfaces, the full simulation cell is a long rectangular prism that includes empty space beyond the surfaces. The full simulation cell is 37.44 Å × 37.44 Å × 150.0 Å.

The interaction potentials were obtained as follows. A B3LYP/6-311G(d,p) geometry optimization of DCTPS was performed using Gaussian09,[29] followed by an evaluation of atomic charges via the CHELPG algorithm.[30] The intramolecular potential for DCTPS was obtained from a series of B3LYP/6-311G(d,p) energies evaluated as the structure of the molecule was systematically varied. Specifically, bending potentials were evaluated from eleven calculations, as the angle is varied within ±10° of the equilibrium angle, torsion potentials were evaluated from 36 energies as the dihedral varies from 0 to 360°, improper torsions are evaluated from 11 energy calculations as the geometry about the central atom is distorted by up-to 10°. For DCTPS, the ring is assumed to be rigid but all stretches, bends, and torsions joining the ring to the propyl group are flexible. An improper torsion potential has been parametrized, based on B3LYP/6-311G(d,p) calculations, and included in the model to maintain planarity of the carbon joining the ring to the propyl group. The full interaction potential also includes OPLS parameters[31,32] for dispersion and short-range repulsion. The solvent models are also flexible: the TraPPE-UA model of *n*-hexane[33] was employed, but the dimethoxypropane model was developed for this work, following the same procedures outlined above for DCTPS.

All simulations are performed with the MDMC program,[34] which includes a parallel implementation of the electrostatic and Lennard-Jones force calculations. Nosé–Hoover thermostats[35,36] have been introduced to maintain a temperature of 298 K. With fixed surface separations, the solvent density within the simulation cell is a function of the number of solvent molecules found between the two surfaces. On the basis of preliminary simulations, we estimated the excluded volume of the surface and adjusted the number of solvent molecules

dx.doi.org/10.1021/jp211503x | J. Phys. Chem. C 2012, 116, 4217–4223

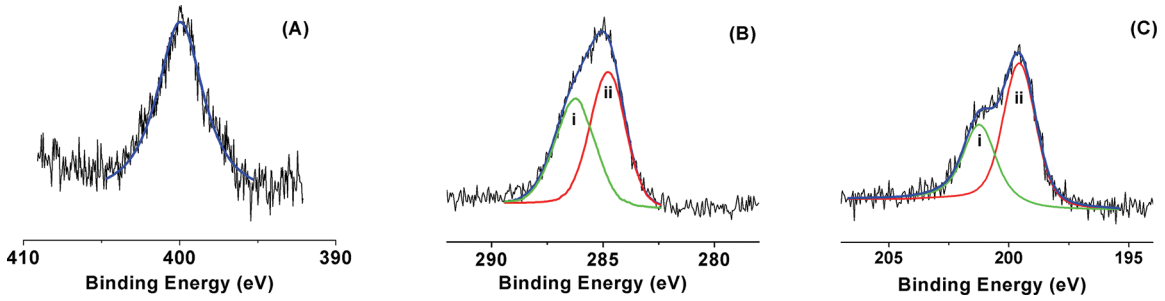

Figure 1. Representative XPS data for (3-(4,6-dichloro-1,3,5-triazin-2-yl)propyl)siloxane films: (A) N(1s), (B) C(1s), and (C) Cl(2p). The black line shows the experimental data, while the blue line is the overall fitted spectrum. In spectrum B, the green trace (i) represents the carbon atoms of the aromatic triazine group, and the red trace (ii) represents the carbon atoms of the aliphatic linker. In spectrum C, the green trace (i) represents chlorine $2p_{1/2}$ and the red trace (ii) chlorine $2p_{3/2}$.

accordingly. For hexane, the final density in the center of the cell is within a few percent of the experimental density, but for 1,3-dimethoxypropane, we find that the effective density at the center of the cell is roughly 10% higher than bulk density at 298 K. The time step in the simulations is 0.3 fs, and two independent simulations have been performed for each interface. Distribution functions are reported for 2.46 ns of simulation time. Ewald summations[37] have been used to treat the electrostatic forces between partially charged atoms.

3. RESULTS AND DISCUSSION

X-ray photoelectron spectroscopy (XPS) was used to characterize (3-(4,6-dichloro-1,3,5-triazin-2-yl)propyl)siloxane overlayers on silicon.[38] The reported binding energy of N 1s in triazine is 399.7 eV[39] and that of an aliphatic amine adjacent to electron withdrawing groups is reported to be 400.1 eV.[40] This relatively small binding energy difference is such that the spectrometer used here cannot distinguish between the two N species. A single N(1s) peak at 400.0 eV is observed, containing contributions from both the triazine and aliphatic amines (Figure 1A). Deconvolution of the C(1s) spectrum using a Powell peak-fitting algorithm with full width at half-maximum (fwhm) of 1.9 eV yields an area ratio of aromatic carbon atoms from the triazine (286.0 eV) and aliphatic carbon atoms from the linker (284.9 eV) of 1.0:1.1, consistent with the 1:1 stoichiometry of (**4**). Deconvolution of the chlorine signal shows peaks at 201.2 eV (Cl $2p_{1/2}$) and 199.6 eV (Cl $2p_{3/2}$) with fwhm of 1.6 eV. Peak area normalization between different elements using relative XPS sensitivity factors as determined by Schofield[41] gives an N/C/Cl ratio equal to 2.0:3.1:1.1. This experimental ratio is close to the expected 2:3:1 stoichiometric ratio. The dichlorotriazine moiety contains both chlorine and nitrogen atoms, so one can imagine that halogen bonding might take place in any 2D film. However, any chemical shift effect associated with this relatively weak, long-range chlorine−nitrogen bonding is likely too small to be observable in any XPS measurement.[42]

Overlayer thicknesses were calculated for the XPS samples as previously reported.[43] Si 2p signal attenuation (I_s/I_0) has been used in this study to estimate the overlayer film thickness using the following relationship:[40]

$$t = (-\lambda \cos \theta) \ln(I_s/I_0)$$

where, t is the thickness of the overlayer, λ is the inelastic mean free path, θ is the takeoff angle (here 15°), I_s is the substrate signal intensity after modification, and I_0 is the substrate signal intensity before modification. The average overlayer thickness was determined to be 0.8 nm. AFM images (Figure 2) show

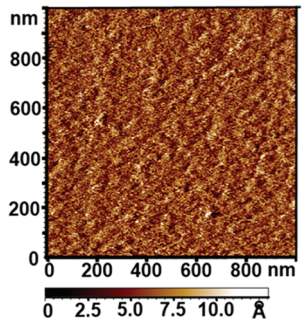

Figure 2. Representative tapping mode AFM image of the 4,6-dichloro-1,3,5-triazin-terminated layer on silicon showing a uniform, smooth layer.

that the film morphology is uniform and smooth with a mean surface roughness for a 1 μm × 1 μm scan area of 0.3 nm. The results of the overlayer thickness measurements and AFM imaging confirm the formation of a uniform surface film of dichlorotriazine. As the film thickness measurements are consistent with the formation of only slightly more than a single overlayer of the (3-(4,6-dichloro-1,3,5-triazin-2-yl)propyl)siloxane, the overall roughness should approximate that of the original unmodified surface. The mean surface roughness of 0.3 nm is in a good agreement with the mean roughness of silicon wafers (0.1−0.46 nm) as observed by AFM.[44]

In order to better understand the potential for this surface to undergo halogen bonding, we performed chemical force (CF) measurements using an AFM tip that is derivatized by the same dichlorotriazine linker. The CF measurements allow us to estimate and compare the influence of different solvents[45] on the forces arising from intermolecular interactions between (3-(4,6-dichloro-1,3,5-triazin-2-yl)propyl)siloxane molecules grafted on the silicon oxide surfaces and deposited on the tip. Alcohols and water, the solvents that are commonly used in CF measurements, cannot be utilized for this system due to reactivity of the cyanuric chloride.

Table 1 lists the average adhesion forces observed in a variety of solvents. For each solvent, we acquired several hundred force−distance curves, at different positions on a single surface. Force curves were reproducible at different points on the surface, demonstrating the homogeneity of the overlayer on the silicon wafer.

The CF measurements in octane and cyclooctane demonstrate negligible force between functionalized surfaces and functionalized tip. This result might be due to significant steric bulkiness of dichlorotriazine moieties and their distribution on the surface. Generally, halogen bonding is characterized

dx.doi.org/10.1021/jp211503x | J. Phys. Chem. C 2012, 116, 4217−4223

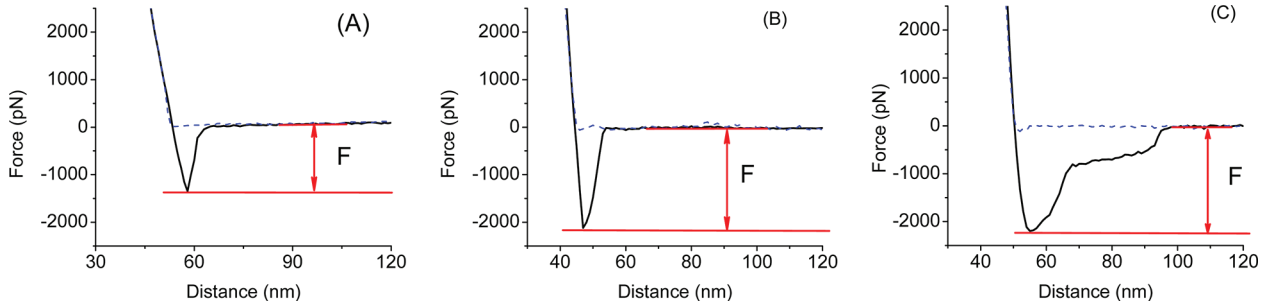

Figure 3. Adhesion forces between dichlorotriazine-terminated surfaces measured in (A) dioxane, (B) diethylene glycol dimethyl ether (DGDE), and (C) triethylene glycol dimethyl ether (TGDE).

Table 1. Adhesion Forces between Tip and Sample Terminated with (3-(4,6-Dichloro-1,3,5-triazin-2-yl)propyl)siloxane in Various Solvents[a]

solvent	adhesion force (nN)
octane	0.05 ± 0.01
cyclooctane	0.02 ± 0.01
carbon tetrachloride	0.08 ± 0.01
trifluoromethyl benzene	0.11 ± 0.01
toluene	0.11 ± 0.02
THF	0.14 ± 0.04
dioxane	1.35 ± 0.06
diethylene glycol dimethyl ether	2.00 ± 0.08
triethylene glycol dimethyl ether	2.07 ± 0.09

[a]The reported errors are the standard deviation for several hundred individual force measurements (see Supporting Information for details).

by (i) a bond distance that should be shorter than the sum of halogen and heteroatom van der Waals radii and (ii) the directionality of the carbon–halogen···heteroatom angle. The carbon–chlorine···nitrogen angle for dichlorotriazine moieties normally varies from 177.59 to 180.00 degrees.[24] This strong directionality of the halogen bond means that the two dichlorotriazine moieties on tip and sample must approach with specific geometry, which may not be possible given that they are conformationally restricted when bound to the surface. Pi-stacking might also be expected to take place between the dichlorotriazine moieties on tip and sample, but here, the directionality considerations would be even more restrictive, and it appears that these interactions cannot be directly observed either.

To overcome this limitation, we performed CF measurements in solvents that themselves may be expected to participate in weak intermolecular interactions with dichlorotriazine moieties. Therefore, we have chosen a series of solvents that may undergo π-stacking or halogen bonding directly with the overlayers without themselves being subjected to severe conformational restraints. Toluene and trifluoromethyl benzene are known to be effective π-stacking participants. It should be noted that π-deficient 1,3,5-triazine rings act as Lewis acids in contrast to π-rich toluene that acts as a Lewis base;[46] thus, the interactions between triazine rings and these solvents are expected to be significant. As seen in Table 1, the interactions between the tip and the surface in these solvents remain quite weak, albeit marginally greater than in octane and cyclooctane. Carbon tetrachloride and tetrahydrofuran have the potential to form halogen bonds with either tip or sample. Again, these forces are similar to those observed for the π-stacking solvents.

The remaining solvents contain two or more potential halogen bonding sites involving oxygen. Like nitrogen, oxygen may halogen bond to chlorine, with a carbon–chlorine···oxygen bond angle of 150.73 to 155.00 degrees.[47−49] This could allow the solvent to bridge between tip and sample. Now, the forces observed become significantly larger. Measurements were carried out in dioxane, diethylene, or triethylene glycol dimethyl ethers (DGDE or TGDE). Dioxane is structurally similar to THF but now contains two O atoms at opposite ends of the molecule. DGDE and TGDE are less bulky and more flexible in comparison with dioxane, while the latter contains three oxygen atoms, increasing the probability of halogen bond formation. Indeed, in dioxane, the forces observed are significantly greater than those seen in THF. In DGDE, the forces are increased even further, consistent with the greater conformational flexibility of this species. Further elongation of the solvent chain by an additional ethylene glycol unit (TGDE) has only a minor influence in the average adhesion force but changes the shape of the force–distance curve (Figure 3), indicating that multiple bonding events between tip and sample occur, due to the multiple O binding sites.

If dioxane molecules serve as linkers between tip and sample, there should be a concentration dependence on the adhesion force observed. Figure 4 shows the dependence of the adhesion

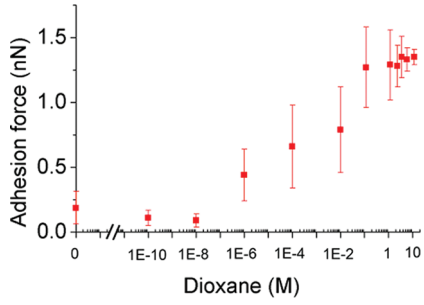

Figure 4. Adhesion forces between dichlorotriazine-terminated surfaces as measured in cyclooctane solutions of varying dioxane concentration.

force on solvent composition for cyclooctane/dioxane solutions. The results are consistent with this, showing that at low concentrations ($<10^{-6}$ M), the adhesion force observed is similar to that in pure cyclooctane, while at higher concentrations ($>10^{-1}$ M), the adhesion forces approach those in pure dioxane. Any further detailed interpretation of the adhesion force dependence on concentration, particularly at intermediate values, is subject to many considerations, including the possibility of solvent partitioning between bulk and surface, so is not pursued further here.

To further demonstrate that oxygen within an ether functionality halogen bonds to the dichlorotriazine, we synthesized 12-morpholinododecane-1-thiol (Scheme 2) and deposited it as

dx.doi.org/10.1021/jp211503x | J. Phys. Chem. C 2012, 116, 4217−4223

Scheme 2. Synthesis of 12-Morpholinododecane-1-thiol [9]

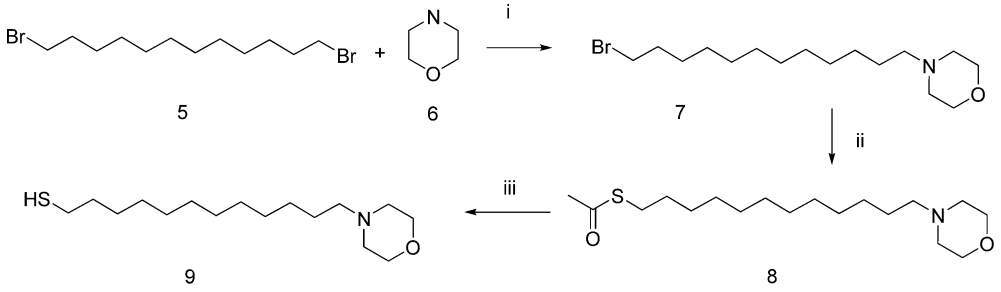

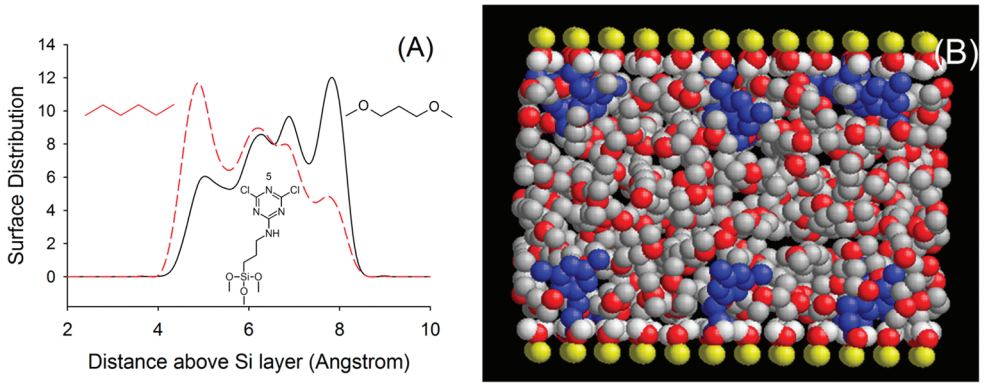

Figure 5. (A) Distribution of N(5) above the surface for 3-(4,6-dichloro-1,3,5-triazin)propyl)siloxane functionalized surfaces separated by 56 Å. The red dashed and the black solid curves show the distribution in *n*-hexane and 1,3-dimethoxypropane respectively. (B) A snapshot for surfaces separated by 42 Å and solvated by 1,3-dimethoxypropane. The rings are shown in blue to emphasize their orientation relative to the surface.

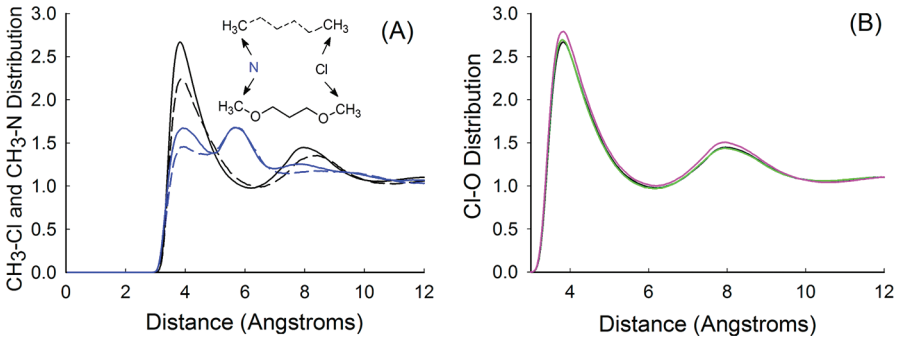

Figure 6. (A) Distribution of terminal methyl groups in 1,3-dimethoxypropane (solid) and *n*-hexane (dashed) with the Cl (black) and central Nitrogen (N(5)) (blue) groups of 3-(4,6-dichloro-1,3,5-triazin)propyl)siloxane functionalized surfaces separated by 56 Å. (B) The distribution between the Cl of 3-(4,6-dichloro-1,3,5-triazin)propyl)siloxane and an oxygen from 1,3-dimethoxypropane as a function of the intersurface separation. The black, green, and pink lines correspond to intersurface separations of 56 Å, 35 Å, and 24 Å, respectively.

a self-assembled monolayer on a gold-coated tip. The terminal ether group of the morpholine moiety may be expected to interact with dichlorotriazine moiety much like the ether groups of dioxane. However, the terminal ether groups of this monolayer are not as flexible as they are for a solution-phase dioxane. The adhesion force measured between a dichloro-triazine-terminated surface and morpholine-terminated tip in cyclooctane was 0.45 ± 0.09 nN. This result is consistent with the formation of a halogen bond involving oxygen and chlorine, while the decrease in force, compared to that in dioxane, may be attributed to conformational restrictions arising from the ether group being tethered to the surface.

Molecular dynamics simulations were performed for (3-(4,6-dichloro-1,3,5-triazin)propyl)siloxane functionalized surfaces separated by 56 Å, 42 Å, 35 Å, 28 Å, and 24 Å. The simulations were conducted in the presence of *n*-hexane or of 1,3-dimethoxypropyl to explore the role of the solvent as the surfaces move closer together.

Figure 5A shows the distribution of N(5), the central nitrogen atom of the ring, above the surface. In either solvent, the nitrogen is found between 4 and 8 Å above the surface. Figure 5B shows a snapshot from a simulation in 1,3-dimethoxypropane where the ring tends to alternate between lying parallel or perpendicular to the surface. In hexane, there is a higher probability of finding the ring parallel to the surface. However, in 1,3-dimethoxypropyl, ring-solvent interactions shift the emphasis toward rings oriented perpendicular to the surface and directed toward the solvent.

The distributions of the terminal methyl group in *n*-hexane and 1,3-dimethoxypropane are compared in Figure 6A. The presence of oxygen in the solvent alters the interaction with the surface; we find that the terminal methyl is more likely to

dx.doi.org/10.1021/jp211503x | J. Phys. Chem. C 2012, 116, 4217–4223

be near the ring chlorines and near N(5) when the solvent is 1,3-dimethoxypropane. This enhanced probability is indicative of stronger interactions between 1,3-dimethoxypropane and the dichlorotriazine ring. The possibility of solvent bridging between surfaces occurs once the surface separation is comparable to the dimensions of a solvent molecule. In Figure 6B, the distribution between the solvent oxygen and the ring chlorine is shown as a function of surface separation. Regardless of surface separation, the oxygen is at least 2.5 times more likely to be near a Cl than would be expected for a randomly distributed solvent. At the shortest separation considered, 24 Å, the surfaces are not quite close enough for a single solvent molecule to bridge the surfaces. Smaller surface separations are difficult to simulate due to an inability to calculate the appropriate number of solvent molecules to include within the gap, as solvent no longer has bulk-like behavior. However, the onset of stronger solvent-surface interactions is apparent by the slightly higher probability of finding an oxygen from 1,3-dimethoxypropane near a ring Cl when the surfaces are only 24 Å apart, as shown in Figure 6B.

Overall, the simulations show that the polar 1,3-dimethoxypropane interacts more strongly with the dichlorotriazine ring than does hexane. Further, the strength of the interaction remains roughly constant until the surfaces are close enough for individual solvent molecules to interact with multiple dichlorotriazine rings. At this point, a slight increase in probability for solvent-ring interactions is observed. The molecular dynamics simulations employ classical, nonpolarizable force fields that cannot capture halogen-bonding. Nonetheless, these simulations do show that the solvent oxygens will be in the vicinity of the ring chlorines and nitrogens, providing a preorientation of the methoxy group that may lead to the formation of halogen bonds.

4. CONCLUSIONS

Weak interactions between surfaces functionalized by (3-(4,6-dichloro-1,3,5-triazin-2-yl)propyl)siloxane were probed by CFS in various solvents. Forces were quite small when measured in alkanes. The force increases slightly when using solvents that are expected to participate in weak interactions with (3-(4,6-dichloro-1,3,5-triazin-2-yl)propyl)siloxane, such as carbon tetrachloride, toluene, trifluoromethyl benzene, and THF. The adhesive force increases significantly if the solvent has multiple oxygens that may serve as halogen bonded linkers between functionalized tip and functionalized surface; adhesion forces increased significantly in dioxane and di- and triethylene glycol dimethyl ether.

■ ASSOCIATED CONTENT

Supporting Information

Materials and methods, synthesis, ^{1}H and ^{13}C NMR data, a representative tapping mode AFM image of functionalized surface, the results of contact angle measurements, and representative force−distance curves. This material is available free of charge via the Internet at http://pubs.acs.org.

■ AUTHOR INFORMATION

Corresponding Author

*Tel: +1 613 533 2379/6704. Fax: +1 613 533 6669. E-mail: Hugh.Horton@chem.queensu.ca.

■ ACKNOWLEDGMENTS

We acknowledge the Natural Sciences and Engineering Research Council of Canada for financial support. A.A.A. acknowledges the financial support of the Skim Latihan Akademik IPTA University of Malaysia Terengganu.

■ REFERENCES

(1) Wuest, J. D. *Chem. Commun.* **2005**, 5830−5837.
(2) Bruce, D. W.; Metrangolo, P.; Meyer, F.; Pilati, T.; Praesang, C.; Resnati, G.; Terraneo, G.; Wainwright, S. G.; Whitwood, A. C. *Chem.—Eur. J* **2010**, *16*, 9511−9524.
(3) Metrangolo, P. R. G. *Science* **2008**, *321*, 918−919.
(4) Lomas, J. S.; Cordier, C.; Adenier, A.; Maurel, F.; Vaissermann, J. *J. Phys. Org. Chem.* **2007**, *20*, 410−421.
(5) Politzer, P.; Lane, P.; Concha, M. C.; Ma, Y.; Murray, J. S. *J. Mol. Modell.* **2007**, *13*, 305−311.
(6) Shirman, T.; Lamere, J.-F.; Shimon, L. J. W.; Gupta, T.; Martin, J. M. L.; van der Boom, M. E. *Cryst. Growth. Des.* **2008**, *8*, 3066−3072.
(7) Cavallo, G.; Metrangolo, P.; Pilati, T.; Resnati, G.; Sansotera, M.; Terraneo, G. *Chem. Soc. Rev.* **2010**, *39*, 3772−3783.
(8) Bertani, R.; Sgarbossa, P.; Venzo, A.; Lelj, F.; Amati, M.; Resnati, G.; Pilati, T.; Metrangolo, P.; Terraneo, G. *Coord. Chem. Rev.* **2010**, *254*, 677−695.
(9) Metrangolo, P.; Carcenac, Y.; Lahtinen, M.; Pilati, T.; Rissanen, K.; Vij, A.; Resnati, G. *Science* **2009**, *323*, 1461−1464.
(10) Lucassen, A. C. B.; Vartanian, M.; Leitus, G.; van der Boom, M. E. *Cryst. Growth Des.* **2005**, *5*, 1671−1673.
(11) Shirman, T.; Freeman, D.; Posner, Y. D.; Feldman, I.; Facchetti, A.; van der Boom, M. E. *J. Am. Chem. Soc.* **2008**, *130*, 8162−8163.
(12) Shirman, T.; Arad, T.; van der Boom, M. E. *Angew. Chem., Int. Ed.* **2010**, *49*, 926−929.
(13) Sarwar, M. G.; Dragisic, B.; Sagoo, S.; Taylor, M. S. *Angew. Chem., Int. Ed.* **2010**, *49*, 1674−1677.
(14) Dyakonenko, V. V.; Maleev, A. V.; Zbruyev, A. I.; Chebanov, V. A.; Desenko, S. M.; Shishkin, O. V. *CrystEngComm* **2010**, *12*, 1816−1823.
(15) Cinčić, D.; Friščić, T.; Jones, W. *Chem. Mater.* **2008**, *20*, 6623−6626.
(16) Gavezzotti, A. *Mol. Phys.* **2008**, *106*, 1473−1485.
(17) Rissanen, K. *CrystEngComm.* **2008**, *10*, 1107−1113.
(18) Yamauchi, Y.; Yoshizawa, M.; Fujita, M. *J. Am. Chem. Soc.* **2008**, *130*, 5832−5833.
(19) Mooibroek, T. J.; Gamez, P. *Inorg. Chim. Acta* **2007**, *360*, 381−404.
(20) Lebel, O.; Maris, T.; Perron, M.-È.; Demers, E.; Wuest, J. D. *J. Am. Chem. Soc.* **2006**, *128*, 10372−10373.
(21) Ebralidze, I. I.; Leitus, G.; Shimon, L. J. W.; Neumann, R. *J. Mol. Struct.* **2008**, *891*, 491−497.
(22) Ebralidze, I. I.; Leitus, G.; Shimon, L. J. W.; Neumann, R. *Inorg. Chim. Acta* **2009**, *362*, 4760−4766.
(23) Xu, K.; Ho, D. M.; Pascal, R. A. *J. Am. Chem. Soc.* **1994**, *116*, 105−110.
(24) Zhu, Y.-M.; Miao, T.-F.; Yang, Y.-Y.; Zhuang, D.-Y.; Zheng, K.-C.; Wong, W.-T. *J. Mol. Struct.* **2010**, *975*, 274−279.
(25) Maruccio, G.; Arima, V.; Cingolani, R.; Liantonio, R.; Pilati, T.; Rinaldi, R.; Metrangolo, P. *CrystEngComm* **2009**, *11*, 510−515.
(26) Lu, Y.; Li, H.; Zhu, X.; Zhu, W.; Liu, H. *J. Phys. Chem. A* **2011**, *115*, 4467−4475.
(27) Noy, A.; Frisbie, C. D.; Rozsnyai, L. F.; Wrighton, M. S.; Lieber, C. M. *J. Am. Chem. Soc.* **1995**, *117*, 7943−51.
(28) van der Boom, M. E.; Evmenenko, G.; Yu, C.; Dutta, P.; Marks, T. J. *Langmuir* **2003**, *19*, 10531−10537.
(29) Frisch, M. J.; Trucks, G. W.; Schlegel, H. B.; Scuseria, G. E.; Robb, M. A.; Cheeseman, J. R.; Scalmani, G.; Barone, V.; Mennucci, B.; Petersson, G. A.; Nakatsuji, H.; Caricato, M.; Li, X.; Hratchian, H. P.; Izmaylov, A. F.; Bloino, J.; Zheng, G.; Sonnenberg, J. L.; Hada, M.; Ehara, M.; Toyota, K.; Fukuda, R.; Hasegawa, J.; Ishida, M.; Nakajima, T.; Honda, Y.; Kitao, O.; Nakai, H.; Vreven, T.;

Montgomery, J. A., Jr.; Peralta, J. E.; Ogliaro, F.; Bearpark, M.; Heyd, J. J.; Brothers, E.; Kudin, K. N.; Staroverov, V. N.; Kobayashi, R.; Normand, J.; Raghavachari, K.; Rendell, A.; Burant, J. C.; Iyengar, S. S.; Tomasi, J.; Cossi, M.; Rega, N.; Millam, J. M.; Klene, M.; Knox, J. E.; Cross, J. B.; Bakken, V.; Adamo, C.; Jaramillo, J.; Gomperts, R.; Stratmann, R. E.; Yazyev, O.; Austin, A. J.; Cammi, R.; Pomelli, C.; Ochterski, J. W.; Martin, R. L.; Morokuma, K.; Zakrzewski, V. G.; Voth, G. A.; Salvador, P.; Dannenberg, J. J.; Dapprich, S.; Daniels, A. D.; Farkas, O.; Foresman, J. B.; Ortiz, J. V.; Cioslowski, J.; Fox, D. J. *Gaussian 09*, revision A.1; Gaussian, Inc.: Wallingford, CT, 2009

(30) Breneman, C. M.; Wilberg, K. B. *J. Comput. Chem.* **1990**, *11*, 361−373.

(31) Briggs, J. M. M. T.; Jorgensen, W. L. *J. Comput. Chem.* **1990**, *11*, 958−971.

(32) Jorgensen, W. L.; Ulmschneider, J. P.; Tirado-Rives, J. *J. Phys. Chem. B* **2004**, *108*, 16264−16270.

(33) Chen, B.; Potoff, J. J.; Siepmann, J. I. *J. Phys. Chem. B* **2001**, *105*, 3093−3104.

(34) Cann, N. M.Unpublished workJared86.

(35) Nosé, S. *J. Chem. Phys.* **1984**, *81*, 511−519.

(36) Hoover, W. G. *Phys. Rev. A* **1985**, *31*, 1695−1697.

(37) Ewald, P. *Ann. Phys., Lpz.* **1921**, *64*, 253−287.

(38) Gulino, A.; Lupo, F.; Condorelli, G. G.; Fragalà, M. E.; Amato, M. E.; Scarlata, G. *J. Mater. Chem.* **2008**, *18*, 5011−5018.

(39) Dieckhoff, S.; Schlett, V.; Possart, W.; Hennemann, O. D. *Fresenius' J. Anal. Chem.* **1995**, *353*, 278−81.

(40) Nelson, G. W.; Perry, M.; He, S.-M.; Zechel, D. L.; Horton, J. H. *Colloids Surf., B* **2010**, *78*, 61−68.

(41) Scofield, J. H. *J. Electron Spectrosc. Relat. Phenom.* **1976**, *8*, 129−37.

(42) Sumii, R.; Sakamaki, M.; Matsumoto, Y.; Amemiya, K.; Kanai, K.; Seki, K. *Surf. Sci.* **2010**, *604*, 1100−1104.

(43) Gulino, A.; Lupo, F.; Fragalà, M. E.; Schiavo, S. L. *J Phys. Chem. C* **2009**, *113*, 13558−13564.

(44) Teichert, C.; MacKay, J. F.; Savage, D. E.; Lagally, M. G.; Brohl, M.; Wagner, P. *Appl. Phys. Lett.* **1995**, *66*, 2346−2348.

(45) Gao, K.; Goroff, N. S. *J. Am. Chem. Soc.* **2000**, *122*, 9320−9321.

(46) Ugozzoli, F.; Massera, C. *CrystEngComm* **2005**, *7*, 121−128.

(47) Trávnícek, Z.; Popa, I. *Acta Crystallogr., Sect. E* **2007**, *63*, o728−o730.

(48) Larson, S. B.; Sanghvi, Y. S.; Revankar, G. R.; Robins, R. K. *Acta Crystallogr. Sect. C: Cryst. Struct. Commun.* **1989**, *45*, 1194−1198.

(49) Chan, D. M. C.; Schwalbe, C. H.; Sood, G.; Fraser, W. *Acta Crystallogr. Sect. C: Cryst. Struct. Commun.* **1995**, *51*, 2383−2386.